HHS Public Access

Author manuscript

Ann Thorac Surg. Author manuscript; available in PMC 2016 March 01.

Published in final edited form as:

Ann Thorac Surg. 2015 March ; 99(3): 770–778. doi:10.1016/j.athoracsur.2014.10.067.

Regional Myocardial Three-Dimensional Principal Strains During Post-Infarction Remodeling

James J Pilla, PhD[1,2], **Kevin J Koomalsingh, MD**[2], **Jeremy R. McGarvey, MD**[2], **Walter RT Witschey, PhD**[1,2], **Larry Dougherty, PhD**[1], **Joseph H. Gorman III, MD**[2], and **Robert C. Gorman, MD**[2]

[1]Department of Radiology, University of Pennsylvania, Philadelphia, PA

[2]Gorman Cardiovascular Research Group, Department of Surgery, University of Pennsylvania

Abstract

Background—The purpose of this study was to quantify myocardial 3D principal strains as the left ventricle (LV) remodels after myocardial infarction (MI). Serial quantification of myocardial strains is important for understanding the mechanical response of the LV to MI. Principal strains convert the 3D LV wall-based strain matrix with 3 normal and 3 shear elements, to a matrix with three non-zero normal elements, thereby eliminating the shear elements which are difficult to physically interpret.

Methods—The study was designed to measure principal strains of the remote, BZ and infarct regions in a porcine model of post- MI LV remodeling. MRI was used to measure function and strain at baseline, one-week, and four-week post-infarct. Principal strain was measured using 3D acquisition and optical flow method (OFM) for displacement tracking.

Results—Principal strains where altered as the LV remodeled. Maximum principal strain magnitude decreased in all regions including the non-infarcted remote while maximum principal strain angles rotated away from the radial direction in the BZ and infarct. Minimum principal strain magnitude followed a similar pattern however strain angles where altered in all regions. Evolution of principal strains correlated with adverse LV remodeling..

Conclusions—Using a state-of-the-art Imaging and OFM technique 3D principal strains can be measured serially after MI in Pigs. Results are consistent with progressive infarct stretching as well as decreased contractile function in the BZ and remote myocardial regions.

Keywords

Remodeling; Principal Strain; MR

Corresponding Author: Robert C. Gorman MD, Perelman School of Medicine, University of Pennsylvania, 3400 Civic Center Blvd, Philadelphia Pa, 19104-5156, Phone: 215-746-4085, Fax: 215-746-2375, Gorman@uphs.upenn.edu.

Introduction

After a myocardial infarction (MI), the left ventricle (LV) is at risk for remodeling. Infarct expansion has been implicated in sustaining LV remodeling after MI [1]. Immediately after ischemia, the infarct region ceases to contract and is subjected to mechanical loads produced by cavity pressure and the non-infarcted remainder of the ventricle. This abnormal loading results in stretching of the infarct and increased stress in the borderzone (BZ) region adjacent to the infarct [2]. This dysfunctional BZ becomes more hypocontractile and progresses to involve additional perfused myocardium as remodeling continues.

Tagged MRI is a method of tracking the myocardial displacement using noninvasive markers [3]. The development of 3D tagging in a single acquisition makes regional LV measurements of the 3D strain possible [4,5]. Principal strains derived from the strain tensor provide information on the magnitude and direction of the deformation that are more amenable to physical interpretation than LV wall-based strains. For LV wall-based strains the strain matrix is oriented with respect to the left ventricular geometry. The coordinate system is rotated so that the x, y, and z direction align with the radial, circumferential, and longitudinal direction of the LV respectively. Components of the normal and shear strains are expressed as magnitudes values in the given wall-based direction. Changes in cardiac strain during remodeling are reported as normal and shear values with constant orientation. Normal strains are easily interpreted while shear strains are more difficult to comprehend because of their definition and complex orientation (Appendix 1).

Studies using invasive methods and tagging have suggested that mechanical changes in the BZ and infarct regions are associated with remodeling [6–8]. These studies have shown that wall-based circumferential and longitudinal strain magnitudes are altered in the infarct and BZ regions. However, a complete understanding of the mechanical alterations in these regions has been limited by the inability to measure 3D strains during remodeling.

The purpose of this study was to serially quantify myocardial 3D principal strains after MI to better understand the mechanism of post MI remodeling.

Material and Methods

The study was designed to quantify the changes in regional principal strains in a porcine model of post-MI remodeling. Animals were treated under an experimental protocol in compliance with NIH “Guide for the Care and Use of Laboratory Animals” (NIH publication 85–23, revised 1996) and approved by the University of Pennsylvania Institutional Animal Care and Use Committee. Five animals received a baseline MRI to access LV volume and regional principal strains prior to infarction. Subsequently, a posterolateral infarct was created by ligating the left circumflex artery distal to the first obtuse marginal artery branch and markers where placed along the boundary of the infarct. The animals were recovered and an MRI was performed at one and four week post-infarction.

MRI was used to measure LV end systolic and end diastolic volume (ESV, EDV), and regional principal strain at baseline, one, and four week after MI using a 3T Scanner

(Siemens, Inc. Malvern, PA). LV volume imaging consisted of a CINE cardiac acquisition followed by strain imaging using a 3D tag sequence [4].

Data Analysis

LV volume data were obtained from the CINE MR images. The endocardial contours were drawn for each slice and phase then imported into a custom program to calculate volumes. Systolic LV regional strain was assessed from tagged images using a method previously described and validated [7]. An optimized 3D optical flow mapping (OFM) algorithm tracked the myocardium motion and produced displacement fields in the x, y, and z direction (Appendix 2). The Lagrangian Green's strain tensor was calculated from the displacement fields between the initial state of ED and the deformed state of ESand principal strains where determined from the strain tensor by solving the eigenvalue problem. Principal strains represent the magnitude (eigenvalue) and direction (eigenvector) of the maximum stretch (E_1), maximum shortening (E_3), and mutually orthogonal difference of the stretch and shortening (E_2) of the myocardium. They differ from wall-based strains by providing a means for tracking not only strain magnitude but strain orientation as the heart remodels. (Appendix 1)

A local wall-based coordinate system was established for eigenvector orientation [9]. The circumferential (***c***) direction was defined by a vector tangent to epicardial contour. Radial direction (***r***) was defined by a vector inward and normal to the local epicardial wall. The longitudinal direction (***l***) was defined to be in the direction of the vector cross product of ***c*** and ***r***, tangent to the epicardial surface. (Figure 1)

Three mid-ventricular slices were selected for quantitative analysis for each animal. To investigate alteration of the principal strains during post-infarction ventricular remodeling, each slice was divided into three segments: infarct, BZ, and remote. Infarct regions were delineated using the markers. The BZ region was determined to be the myocardium encompassed by a 20° arc between the marker and the remote region [10].

Statistics

Data are presented as mean ± SEM. LV volume data were assessed using one-way repeated measures ANOVA with Tukey post-hoc evaluation. Two-way repeated measures ANOVA with Tukey multiple comparisons was used to analyze the principal strain for differences between regions and time points. Pearson and Spearman's ranked-order correlation where used to analyze the relationship between the change in regional strain and LV volume. Strain magnitudes and directions in each segment were compared by paired Student's t-test. $P < 0.05$ was considered statistically significant for all comparisons.

Results

Global LV Remodeling

Global LV remodeling occurred in all animals throughout the study period. Statistically significant and progressive increases in EDV and ESV were documented as was a concurrent decrease in EF. (Table 1)

Principal Strains

Representative 3D tagged images are shown in Figure 2. Altered deformation of the tags in the infarct and BZ regions is evident at ES. Maximum, minimum, and intermediate principal strains are presented below for each region and time point.

Maximum Principal Strain—The magnitude (eigenvalue – E_1Mag) and direction (eigenvectors – $E_1\theta_{RC}$, $E_1\theta_{RL}$, $E_1\theta_{CL}$) of the maximum principal strain (E_1) for the cohort of animals are presented in Figure 3. At baseline, the magnitude of the E_1 is similar in all regions (Figure 3A). $E_1\theta_{RC}$ (Figure 3B) and $E_1\theta_{RL}$ (Figure 3C) measure the angles between local radial direction and the projection of E_1 on to transverse and longitudinal plane, respectively. Both $E_1\theta_{RC}$ (Figure 3B) and $E_1\theta_{RL}$ (Figure 3C) before infarction are less than 10° while $E_1\theta_{CL}$ is near 45° (Figure 3D) for all regions, demonstrating that before infarction E_1 is directed predominately in the radial direction indicative of normal wall thickening.

One and 4 weeks post-MI the magnitude of E_1 (i.e. E_1Mag) is significantly reduced in all myocardial regions (Figure 3A). Interpretation of this reduced magnitude is highly dependent on the associated changes in eigenvector directions: $E_1\theta_{RC}$, $E_1\theta_{RL}$ and $E_1\theta_{CL}$. Reduction in E_1Mag can be interpreted as a decrease in radial wall thickening if the associated eigenvector directions angles are not significantly changed from the baseline values (i.e. $E_1\theta_{RC}$, and $E_1\theta_{RL}$ near zero; $E_1\theta_{CL}$ near 45°).However, changes in the associated eigen vector directions, especially increases in $E_1\theta_{RC}$ and $E_1\theta_{RL}$, are indicative of some degree regional myocardial stretching.

One-week post-MI, the eigenvector of E_1 in the BZ and infarct regions deviate from the original radial direction, resulting in significant increase in $E_1\theta_{RC}$ with the infarct having the largest change. $E_1\theta_{CL}$ decreases in both the BZ and infarct regions. These changes are consistent with a shift from radial thickening to circumferential stretching. $E_1\theta_{RL}$ is unchanged in BZ but increases in the infarct indicating a shift from radial thickening to longitudinal stretch in this region. All angles in the remote region are unchanged at 1 week after MI; however, E_1Mag in this region is significantly reduced indicating reduced wall thickening.

Four weeks after MI, the eigenvector for E_1 in the infarct continues to deviate from the radial direction as indicated by the continued increases in $E_1\theta_{RC}$ and $E_1\theta_{RL}$. These data are consistent with progressive circumferential and longitudinal infarct stretching as well as complete loss of wall thickening in the infarct region. In the BZ E_1Mag remains decreased and all three angles are increased, which is consistent with decreased wall thickening and increased circumferential and longitudinal stretching. In the remote region all angles remain preserved, but there is a persistent reduction in E_1Mag indicating that remote wall thickening remains impaired at 4 weeks after MI.

Minimum Principal Strain—The magnitude (eigenvalue – E_3Mag) and direction (eigenvectors - $E_3\theta_{RC}$, $E_3\theta_{RL}$ and $E_3\theta_{CL}$) of the minimum principal strain (E_3) for the cohort of animals are presented in Figure 4. Before infarction E_3Mag is similar in all regions. $E_3\theta_{RC}$ and $E_3\theta_{RL}$ approach 90° at baseline while $E_3\theta_{CL}$ is near 45° (Figure 4B, 4C and 4D). These eigenvec tors indicate that the majority of myocardial shortening occurs in the

circumferential and longitudinal directions. The orientation of $E_3\theta_{CL}$ is also indicative of a spiraling or torsional contraction from apex to base (Figure 4D). The physical interpretation of these findings is that before infarction the minimum principal strain (E_3) represents the maximum shortening or contraction in the LV wall. During systole the normal LV simultaneously shortens in both the longitudinal and circumferential directions which contribute to the well-described torsional movements of the LV. [11, 12].

One week after MI all regions demonstrate decreased E_3, with the infarct region having the lowest strain (Figure 4A). The infarct region also exhibits a significant decrease in $E_3\theta_{RC}$ indicating a shifting from circumferential shortening to radial shortening. $E_3\theta_{RL}$ is significantly reduced in all regions due to a change in shortening orientation away from the longitudinal direction. At 4 weeks after MI, E_3Mag in all regions increases relative to 1 week, but fails to reach pre-infarction levels. The increased E_3Mag in the remote region may be jointly attributed to contractile compensation as well as increased infarct compliance which theoretically could decrease initial resistance to contraction. Whereas in the infarct the increase in E_3Mag is indicative of increased stretch and in the BZ it is likely a combination of both contractile compensation and increased stretch. Additionally, at 4-weeks $E_3\theta_{RC}$ and $E_3\theta_{RL}$ in the infarct remain significantly reduced relative to pre-infarction which is indicative of persistent atypical shortening in the radial direction (i.e. continued infarct systolic thinning). BZ region continued to have altered strain in both $E_3\theta_{RL}$ and $E_3\theta_{CL}$. The remote region returned to baseline $E_3\theta_{RL}$ values while, $E_3\theta_{CL}$ continued to be elevated signifying altered torsion.

Bulls-eye plots of the minimum and maximum principal strain eigenvalues and eigenvector components for a representative animal are shown in figure [5A and 5B].

Intermediate Principal Strains—The physical interpretation of intermediate principal strain (E_2) is more difficult to determine. While E_1 and E_3 represent the thickening and shortening respectively, E_2 is the mutually perpendicular strain to E_1 and E_3. Following infarction significant changes occur in E_2 (Figure 6A). $E_2\theta_{RC}$ is altered at 4 weeks after infarction with little change in the remote and BZ (Figure 6B). $E_2\theta_{RL}$ is decreased at one week and four weeks after MI (Figure 6C).

Correlation of Principal Strain with LV Remodeling

One-week post-MI the change in EDV from baseline was correlated with changes in several of the principal strain components. E_1 components in both the remote and infarct regions where highly correlated while components in the BZ and infarct where better correlated for E_3. ESV change was also correlated to components of both E_1 and E_3 (Table 2).

E_3 was the only principal strain correlated with remodeling at four weeks post infarct (Table 3). EDV was correlated with eigenvector angles for both the remote and BZ while changes in ESV where associated with angles in the infarct and BZ regions.

Principal strains at one-week where compared to the change in LV remodeling from one-week to four-weeks as a potential predictor of remodeling (Table 4). E_3 infarct had a strong positive correlation with increasing EDV as the LV continued to remodel. Angular

components of E_1 in the remote region also demonstrated an influence on dilatation. ESV dilatation was strongly negatively correlated to E_2 infarct and E_1 remote and positively correlated a maximum principal strain angle in the infarct region. Ejection fraction was correlated to the magnitudes of E_1 in the BZ and E_2 in the remote region as well as an angular component of E_1 infarct.

Comment

In this study we employed an optical flow method (OFM) [4] as well as an acquisition scheme that enables direct measurement of 3D myocardial displacement before and after a posterolateral MI in pigs. Using this combined acquisition and tracking method we quantified the temporal changes in the 3D strain tensor to gain an improved understanding of the evolution of post-infarct remodeling.

Our results indicated that during LV remodeling strain was altered in all regions and at all time-points after MI with the most pronounced changes occurring in the BZ and infarct regions. Previous ex vivo tissue experiments have demonstrated that infarct passive mechanical stiffness is greatest at 1-week after coronary occlusion and decreases progressively with time leading to increased tissue stretch [13]. This temporal change in infarct material properties is confirmed by the magnitude and orientation of the eigenvectors presented in this study. One week after MI, the orientation of the E_1 eigenvectors demonstrate that the infarct is stretching in the longitudinal and circumferential direction rather than thickening in the radial direction. Four weeks after MI, the orientation of the E_1 eigenvectors indicate progressive stretch in longitudinal and circumferential directions consistent with a continued decrease in infarct stiffness. Concomitant post-infarction changes in the orientation of the E_3 eigenvectors are indicative of progressive systolic wall thinning and confirm progressive loss of infarct stiffness during post-MI LV remodeling.

The changes in principal strain magnitude and angles over time are indicative of the active role the infarct mechanical properties play in LV remodeling and function. Rapid loss of contractile function after coronary occlusion immediately reduces the systolic compliance of the infarct. Over time the infarct stiffness decreases further, which increases infarct strain (stretching) and wall stress as the infarct becomes more compliant. Progressive infarct compliance increases the workload of the remote myocardium by increasing the work lost to stretching in the infarct region [14]. Increased LV wall stress has also been associated with maladaptive biologic sequelae particularly matrix metalloproteinase activation. [15]

BZ which is classified as the hypokinetic region adjacent to the infarct is under unique stress due to its position between the normally contracting remote myocardium and the non-contractile infarct [2]. This region undergoes a comparable temporal evolution of strain magnitude and angles as the infarct region even though it is not part of the initial ischemic insult. E_1Mag decreases early and remains depressed at the late time point. Angles are rotated away from the pre-infarct radial direction but to a lesser degrees than the infarct region suggesting there is a component of BZ thickening in the radial direction and a portion is stretching in both the longitudinal and circumferential directions. These observed

temporal changes in BZ strain can be attributed to the altered stress distribution due the adjacent infarct region and are potentially a stimulus for continued remodeling [16, 17].

Remote principal strain magnitudes decreased at one week after MI, and then subsequently increased at 4-weeks. Improved strain in the remote region may be jointly attributed to contractile compensation and increased infarct compliance. Infarct stretch lessens initial contractile load increasing the remote strain; however, this results in increased LV workload for a given stroke volume [14].

The orientation E_1 eigenvectors ($E_1\theta_{RC}$, $E_1\theta_{RL}$ and $E_1\theta_{CL}$) in the remote region changed little after MI indicating myocardial thickening continued to be predominantly in the radial direction. Minimum principal strain angles where altered in the remote with remodeling, signifying that shortening had rotated away from the longitudinal direction to more circumferential orientation. This rotation was likely a consequence of reduced LV torsion [18, 19]. Decreased torsion due to the non-contracting infarct region would impair the LV's ability to shorten in the longitudinal direction altering the longitudinal components (θ_{RL} and θ_{CL}) of E_3. This decreased shortening would increase myocardial stress and oxygen demand by increasing LV workload and could contribute to continue remodeling and decreased function [14, 20].

An appreciation of the temporal changes in LV wall principal strains after MI is crucial to understanding the mechanism of LV remodeling as well as to developing new strategies to halt or reverse the process. Altering the principal strains in the infarct and BZ has become a potential therapeutic target to prevent the progression of LV remodeling after MI. Mechanical and biological methods of modifying stress/strains in the infarct have been proposed. These include restraint devices [21, 22] placed over the infarct and stiffening agents injected [23, 24] into the infarct tissue. The successful application of these novel therapeutic approaches will be dependent on a better understanding of the time-dependent changes that occur in healing and mature MI

This study also examined the prognostic value of principal strains in predicting remodeling. Correlation studies between the evolution of principal strain and adverse LV remodeling demonstrate that regional magnitude and angles have prognostic significance indicating that principal strain changes precede ventricular dilatation and performance decline. Previous studies using 2D echo measuring normal strains have concluded that global circumferential and longitudinal strains were predictive of adverse remodeling after MI [25–27]. These global strain changes are a consequence of the regional alterations. Infarct and BZ principal strains will influence the strains over the entire LV by modifying systolic and diastolic stress distribution and blood flow patterns. Regional principal strain may be a more powerful predictor since remodeling post-MI likely begins on the regional level then affects the ventricle globally.

Principal strain orientation maybe less affected by preload and afterload especially in the infarct and BZ regions. Strain orientation in these regions is more a function of material properties than contractile load. Accordingly, regional principal strains maybe a better

predictor of which patients will benefit from emerging infarct modification therapies as well as determining the optimal timing for such interventions.

Supplementary Material

Refer to Web version on PubMed Central for supplementary material.

References

1. Jackson BM, Gorman JH III, Moainie SL, et al. Extension of Borderzone Myocardium in Post Infarction Dilated Cardiomyopathy. J Am Coll Cardiol. 2002; 40:1160–1167. [PubMed: 12354444]
2. Jackson BM, Gorman JH 3rd, Salgo IS, et al. Border zone geometry increases wall stress after myocardial infarction: contrast echocardiographic assessment. Am J Physiol Heart Circ Physiol. 2003 Feb; 284(2):H475–H479. [PubMed: 12414441]
3. Axel L, Dougherty L. MR imaging of motion with spatial modulation of magnetization. Radiology. 1989; 171:841–845. [PubMed: 2717762]
4. Xu C, Pilla JJ, Isaac G, et al. Deformation analysis of 3D tagged cardiac images using an optical flow method. Cardiovasc Magn Reson. 2010 Mar.30:12–19.
5. Zhong X, Spottiswoode BS, Meyer CH, et al. Imaging three-dimensional myocardial mechanics using navigator-gated volumetric spiral cine DENSE MRI. Magnetic Resonance in Medicine. 2010; 64:1089–1097. [PubMed: 20574967]
6. Zimmerman SD, Criscione J, Covell JW. Remodeling in myocardium adjacent to an infarction in the pig left ventricle. Am J Physiol Heart Circ Physiol. 2004; 287:H2697–H2704. [PubMed: 15319211]
7. Cupps BP, Pomerantz BJ, Krock MD, et al. Principal Strain Orientation in the Normal Human Left Ventricle. Ann Thorac Surg. 2005; 79:1338–1343. [PubMed: 15797074]
8. Blom AS, Pilla JJ, Arkles J, et al. Ventricular Restraint Prevents Infarct Expansion and Improves Borderzone Function After Myocardial Infarction: A Study Using Magnetic Resonance Imaging, Three-Dimensional Surface Modeling, and Myocardial Tagging. Ann Thorac Surg. 2007; 84:2004–2010. [PubMed: 18036925]
9. Moore CCMD, Lugo-Olivieri CH, McVeigh ER, et al. Radiology. Three-dimensional Systolic Strain Patterns in the Normal Human Left Ventricle: Characterization with Tagged MR Imaging. Radiology. 2000; 214(2):453–466. [PubMed: 10671594]
10. Pilla JJ, Blom AS, Gorman JH 3rd, et al. Early postinfarction ventricular restraint improves borderzone wall thickening dynamics during remodeling. Ann Thorac Surg. 2005 Dec; 80(6): 2257–2262. [PubMed: 16305885]
11. Rüssel IK, Götte MJ, Bronzwaer JG, et al. Left ventricular torsion: an expanding role in the analysis of myocardial dysfunction. JACC Cardiovasc Imaging. 2009 May; 2(5):648–655. [PubMed: 19442954]
12. Buchalter MB, Weiss JL, Rogers WJ, et al. Noninvasive quantification of left ventricular rotational deformation in normal humans using magnetic resonance imaging myocardial tagging. Circulation. 1990 Apr; 81(4):1236–1244. [PubMed: 2317906]
13. Gupta KB, Ratcliffe MB, Fallert MA, et al. Changes in passive mechanical stiffness of myocardial tissue with aneurysm formation. Circulation. 1994 May; 89(5):2315–2326. [PubMed: 8181158]
14. Pilla JJ, Gorman JH 3rd, Gorman RC. Theoretic Impact of Infarct Compliance on Left Ventricular Function. Ann Thorac Surg. 2009 Mar; 87(3):803–810. [PubMed: 19231393]
15. Wilson EM, Moainie SL, Baskin JM, et al. Region and Type Specific Induction of Matrix Metalloproteinases in Post Myocardial Infarction Remodeling. Circulation. 2003; 107:2857–2863. [PubMed: 12771000]
16. Guccione JM, Moonly SM, Moustakidis P, et al. Mechanism underlying mechanical dysfunction in the border zone of left ventricular aneurysm: a finite element model study. Ann Thorac Surg. 2001 Feb; 71(2):654–662. [PubMed: 11235723]

17. Moustakidis P, Maniar HS, Cupps BP, et al. Altered left ventricular geometry changes the border zone temporal distribution of stress in an experimental model of left ventricular aneurysm: a finite element model study. Circulation. 2002 Sep 24; 106(12 Suppl 1):I168–I175. [PubMed: 12354728]

18. Nucifora G, Marsan NA, Bertini M, et al. Reduced left ventricular torsion early after myocardial infarction is related to left ventricular remodeling. Circ Cardiovasc Imaging. 2010 Jul; 3(4):433–442. [PubMed: 20478987]

18. Jang JY, Woo JS, Kim WS, et al. Serial assessment of left ventricular remodeling by measurement of left ventricular torsion using speckle tracking echocardiography in patients with acute myocardial infarction. Am J Cardiol. 2010 Oct 1; 106(7):917–923. [PubMed: 20854950]

20. Beyar R, Sideman S. Left ventricular mechanics related to the local distribution of oxygen demand throughout the wall. Circ Res. 1986 May; 58(5):664–677. [PubMed: 3708764]

21. Koomalsingh KJ, Witschey WR, McGarvey JR, et al. Optimized local infarct restraint improves left ventricular function and limits remodeling. Ann Thorac Surg. 2013 Jan; 95(1):155–162. [PubMed: 23146279]

22. Pilla JJ, Blom AS, Brockman DJ, et al. Ventricular constraint using the acorn cardiac support device reduces myocardial akinetic area in an ovine model of acute infarction. Circulation. 2002 Sep 24; 106(12 Suppl 1):I207–I211. [PubMed: 12354735]

23. Ryan LP, Matsuzaki K, Noma M, et al. Dermal filler injection: a novel approach for limiting infarct expansion. Ann Thorac Surg. 2009 Jan; 87(1):148–155. [PubMed: 19101288]

24. Ifkovits JL, Tous E, Minakawa M, et al. Injectable Hydrogel Properties Influence Extent of Post-Infarction Left Ventricular Remodeling in an Ovine Model. Proceedings of the National Academy of Science. 2010; 107:11507–11512. 2010.

25. Hung CL, Verma A, Uno H, et al. Longitudinal and circumferential strain rate, left ventricular remodeling, and prognosis after myocardial infarction. J Am Coll Cardiol. 2010 Nov 23; 56(22): 1812–1822. [PubMed: 21087709]

26. Cho GY, Marwick TH, Kim HS, et al. Global 2-dimensional strain as a new prognosticator in patients with heart failure. J Am Coll Cardiol. 2009 Aug 11; 54(7):618–624. [PubMed: 19660692]

27. Su HM, Lin TH, Hsu PC. Global left ventricular longitudinal systolic strain as a major predictor of cardiovascular events in patients with atrial fibrillation. Heart. 2013 Nov; 99(21):1588–1596. [PubMed: 24014280]

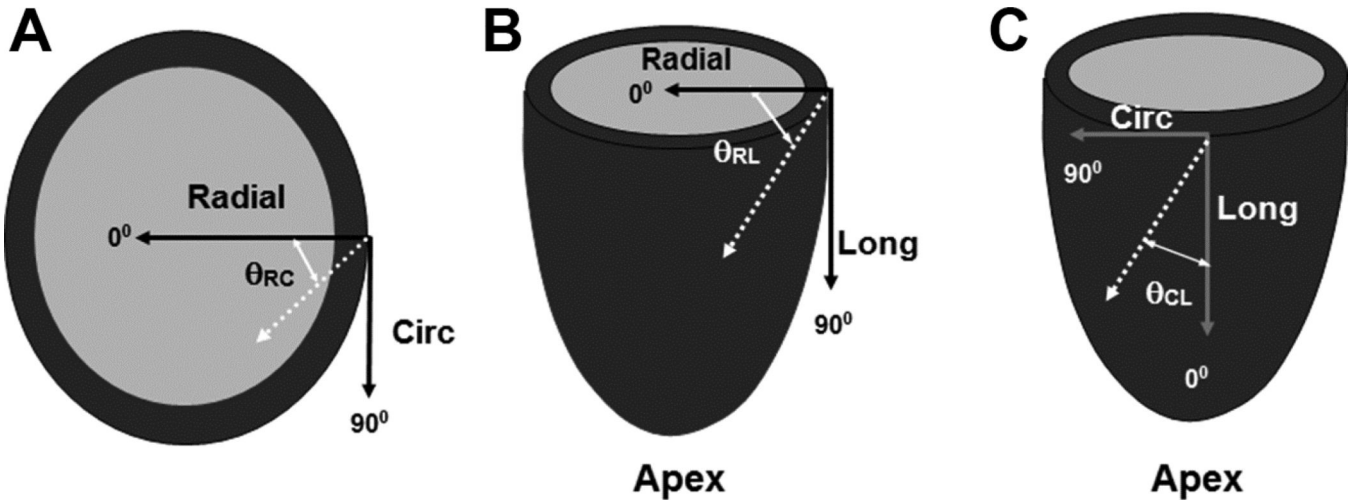

Figure 1. Coordinate System of Principal Strain Vectors

Radial-circumferential angle (θ_{RC}) is the principal strain vector projected on the radial/ circumferential plane (A). Analogous descriptions are used for the radiallongitudinal (θ_{RL}) (B) and longitudinal-circumferential (θ_{CL}) planes (C). (**Long**: longitudinal, **Circ**: circumferential)

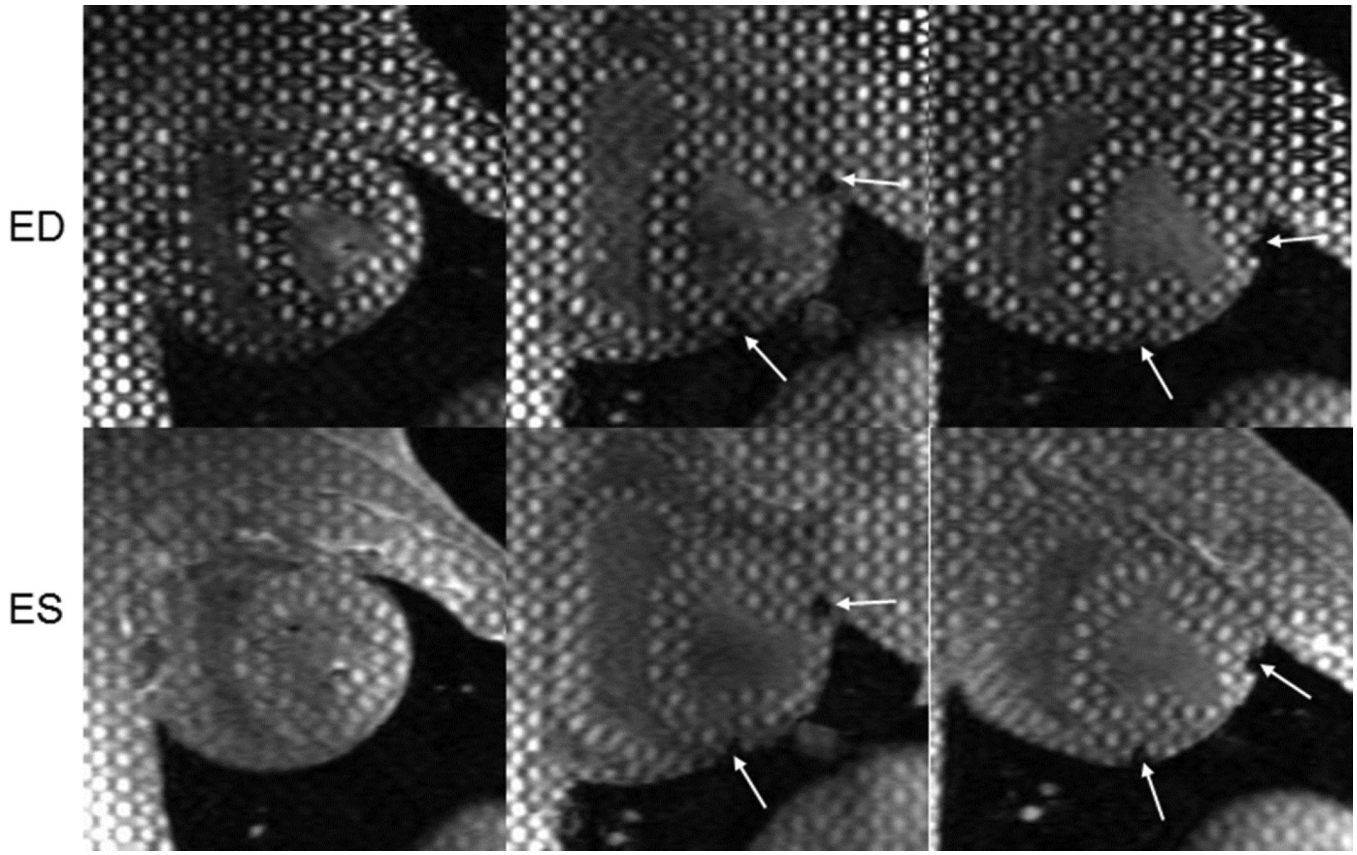

Figure 2. Tagged images of left ventricular (LV) remodeling following MI

Short-axis mid-ventricular images acquired at baseline (left), 1-week (middle), and 4-weeks (right) after infarct. End-diastolic (ED) images (top row) show the change in LV size and geometry with infarct progression. Regional tag deformation at end-systole (ES) are shown for the three time points in the bottom row. Infarct region is delineated using markers which create signal voids (arrows).

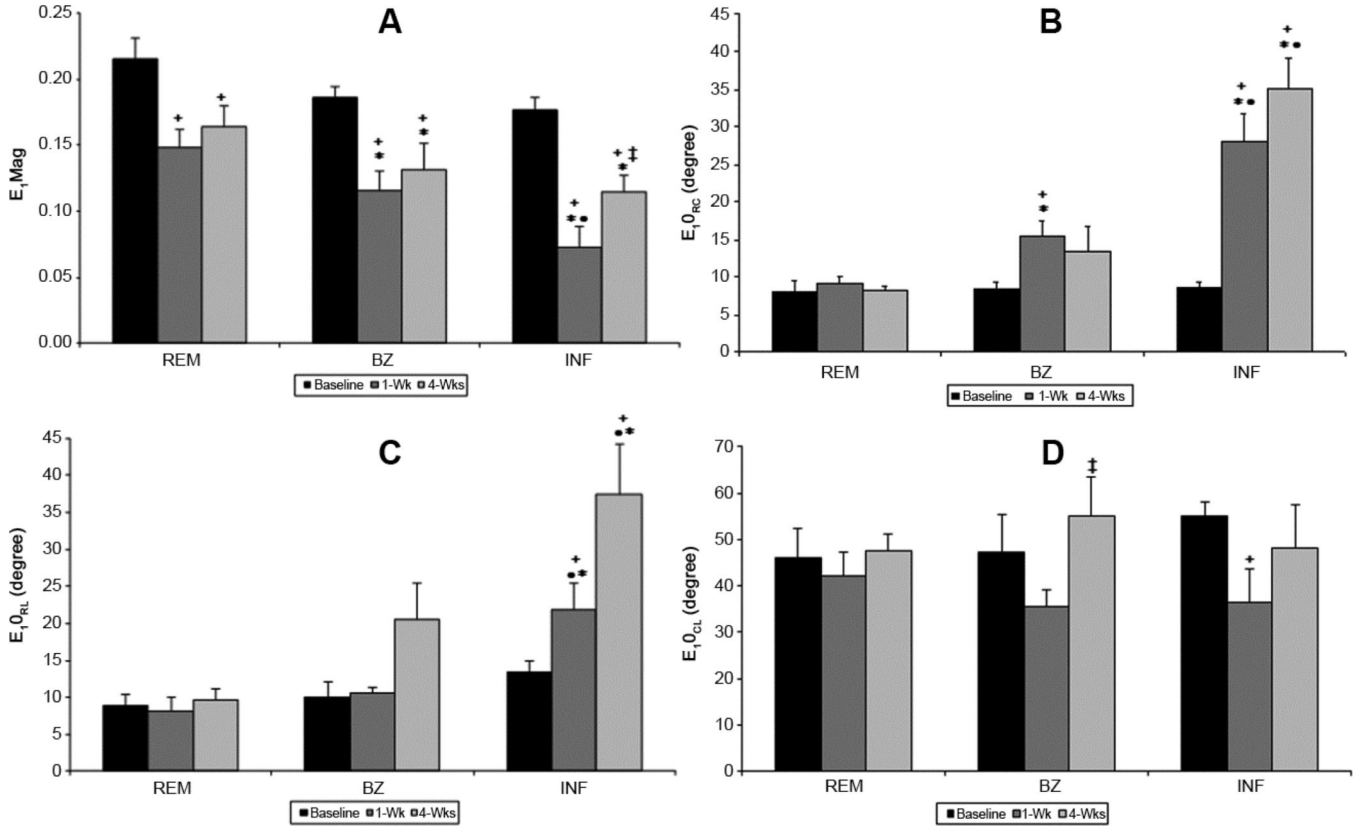

Figure 3. Regional maximum principal strain magnitude and angles during LV remodeling

Maximum principal strain magnitude (E_1Mag) is altered in all regions as the ventricle remodels. Infarct (INF) experiences the greatest change in E1Mag, decreasing at 1-wk then increasing at 4-wks. Maximum principal strain angles ($E_1\theta_{RC}$, $E_1\theta_{RL}$, $E_1\theta_{CL}$) where unchanged in the remote region. Infarct and borderzone (BZ) angles rotated away from the radial direction to a more circumferential-longitudinal direction indicating stretch. (+ $p<0.05$ vs baseline, ‡ $p<0.05$ vs 1wk, *$p<0.05$ vs REM, • <0.05 vs BZ)

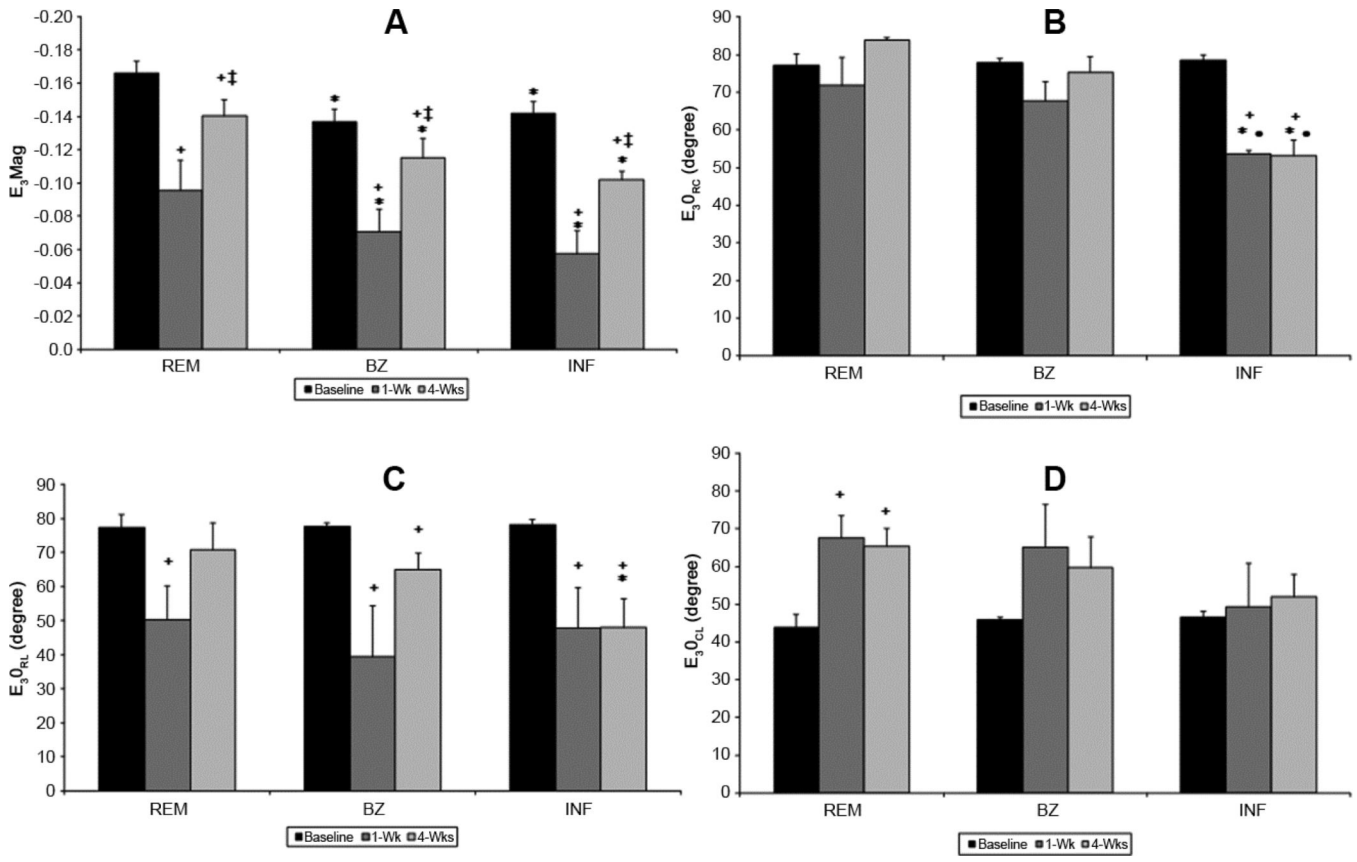

Figure 4. Regional minimum principal strain magnitude and angles during LV remodeling

At 1-week (1-wk) minimum principal strain magnitude (E_3Mag) decreases in all regions but increases as remodeling continues. Remote (REM) improvement could be attributed to LV compensation whereas borderzone (BZ) and infarct (INF) increase is probably a consequence of tissue stretch. Angles ($E_1\theta_{RC}$, $E_1\theta_{RL}$, $E_1\theta_{CL}$ are altered in all regions which may be attributed to both changes in INF and BZ tissue properties and decreased LV torsion. (+ $p<0.05$ vs baseline, ‡ $p<0.05$ vs 1wk, *$p<0.05$ vs REM, • <0.05 vs BZ)

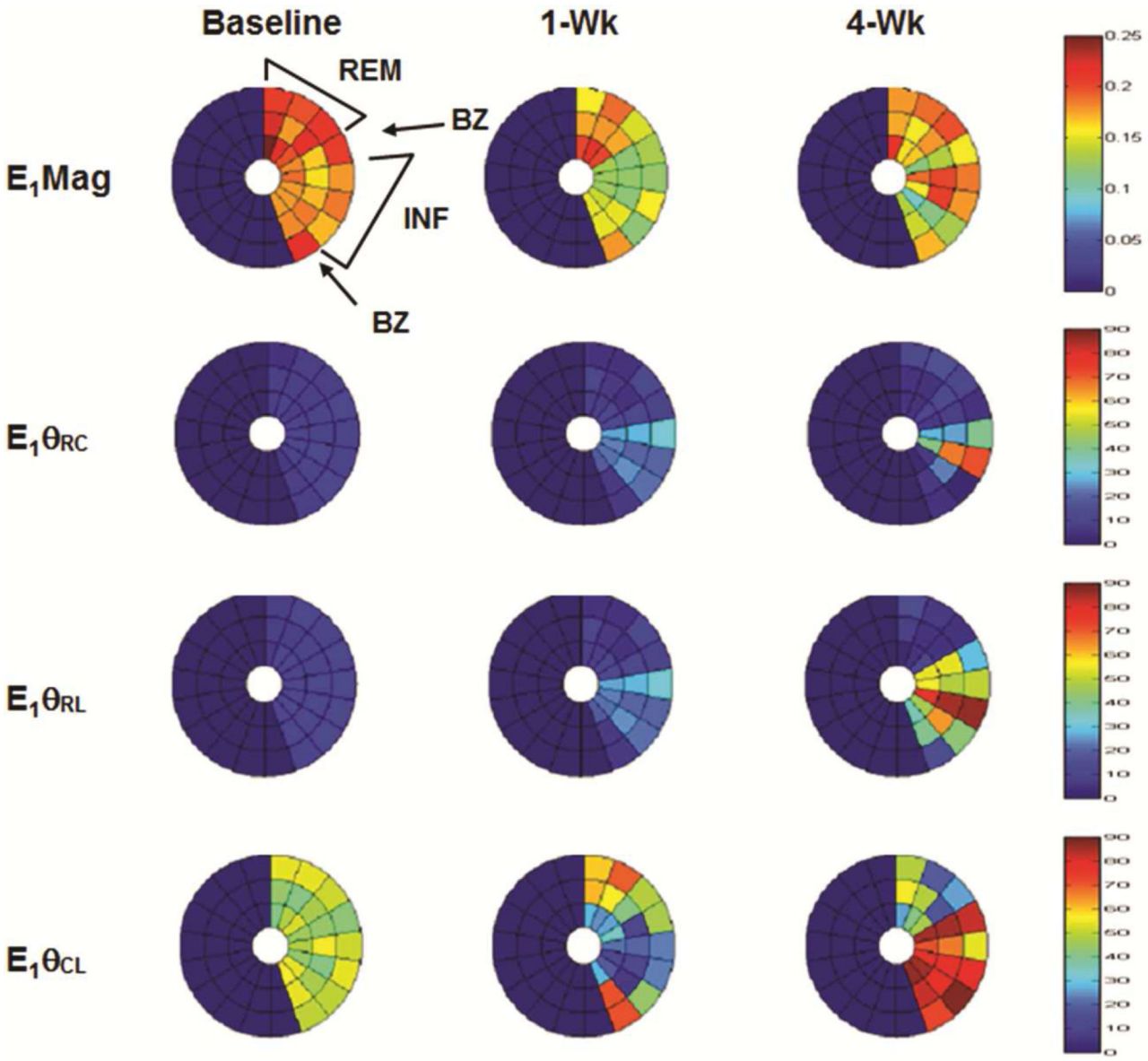

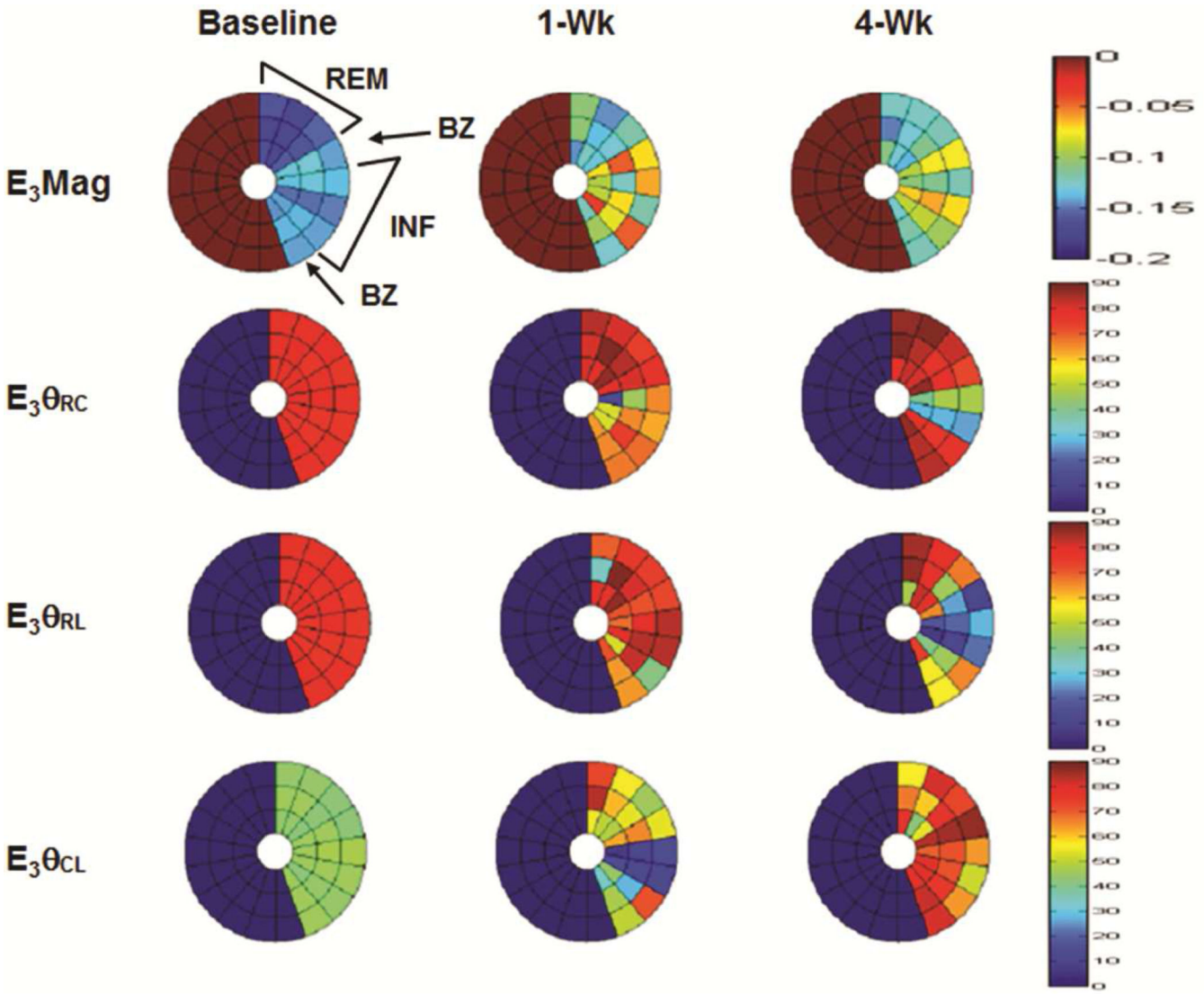

Figure 5. Bulls-eye plots of maximum (E_1) (A) and minimum (E_3) (B) principal strain at baseline, one week (1-Wk) and four week (4-Wk) post-infarct for a representative animal

Plots display three mid-ventricular slices from apex (inner) to base (outer) for remote (REM), border zone (BZ), and infarct (INF) regions. E_1 magnitude (E_1Mag) decreases in all regions at 1-Wk but increases at 4-wks in the infarct. Infarct E_1 vectors ($E_1\theta_{RC}$, $E_1\theta_{RL}$) shift from radial direction at baseline to more circumferential/longitudinal signifying decreased wall thickening and increased tissue stretch. Circumferential shortening (E_3Mag) decreases in all regions as the LV remodels while infarct E_3 vectors shifts ($E_3\theta_{RC}$, $E_3\theta_{RL}$) from circumferential/longitudinal to a more radial direction indicating tissue stretch.

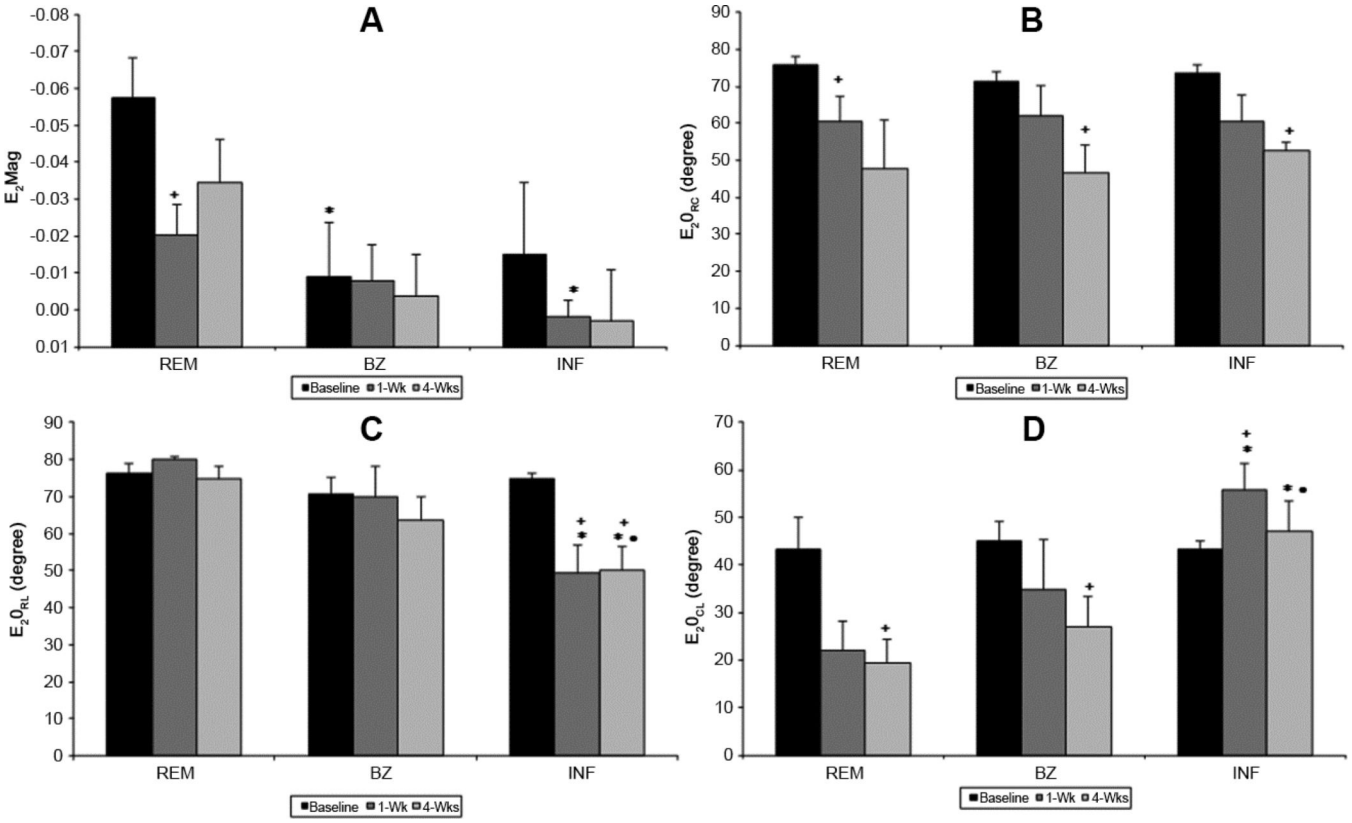

Figure 6. Regional intermediate principal strain magnitude and angles during LV remodeling

Contrasting E_1Mag and E_3Mag, the regional magnitude of E_2 (E_2Mag) varies significantly with location before infarction. Following infarction $E_2\theta_{RC}$ is altered at 4 weeks with little change in the remote (REM) and borderzone (BZ). $E_2\theta_{RL}$ is decreased at one week and four weeks after MI. (+ $p<0.05$ vs baseline, *$p<0.05$ vs REM, • <0.05 vs BZ)

Table 1

Change LV function with remodeling

	Baseline	1-week	4-weeks
EDV (ml)	61.4±4.7	90.4±8.7*	119.9±11.8†
ESV (ml)	34.7±3.6	58.9±5.1*	84.1±8.3†
EF (%)	43.3±2.5	34.7±1.4*	29.7±3.2†

Mean ± SEM

* p<0.05 vs. baseline,

† p<0.05 vs. 1-week.

Table 2

Correlation between function and principal strain at one-week

	Principal Strain	R value	p
EDV	$E_1\theta_{RC}$remote	0.85	0.06
	$E_1\theta_{RC}$infarct	0.90	0.03
	E_3BZ	0.82	0.08
	$E_3\theta_{RC}$BZ	−1	0.01
	$E_3\ \theta_{CL}$infarct	−1	0.01
ESV	$E_1\theta_{RC}$remote	0.81	0.09
	$E_1\theta_{RC}$infarct	−0.86	0.05
	E_1BZ	0.92	0.02
	E_3BZ	0.90	0.08
	$E_3\theta_{RC}$BZ	−1	0.01

Table 3

Correlation between function and principal strain at four-week

	Principal Strain	R value	p
EDV	$E_3\theta_{RL}$remote	0.90	0.08
	$E_3\theta_{CL}$BZ	−0.90	0.08
ESC	$E_3\theta_{RL}$BZ	0.85	0.07
	$E_3\theta_{CL}$BZ	−0.81	0.09
	$E_3\theta_{RL}$infarct	0.90	0.08
	$E_3\theta_{CL}$infarct	−0.84	0.07

Table 4

Correlation between principal strain at one-week and function from one-week to four-week

	Principal Strain	R value	p
EDV	$E_1\theta_{RL}$remote	−0.88	0.04
	$E_1\theta_{CL}$remote	−0.81	0.09
	E_3infarct	0.92	0.02
ESV	E_1remote	−0.94	0.01
	$E_1\theta_{CL}$infarct	0.94	0.01
	E_2infarct	−0.98	0.003
EF	E_1BZ	0.83	0.08
	$E_1\theta_{RL}$infarct	−0.86	0.06
	E_2remote	−0.90	0.02